Journal of Applied Polymer Science

Enhanced adsorption and recovery of Pb(II) from aqueous solution by alkali-treated persimmon fallen leaves

Ruiyi Fan,[1] Qingping Yi,[1,2] Yucong Xie,[1] Feng Xie,[3] Qinglin Zhang,[1,4] Zhengrong Luo[1,4]

[1]Key Laboratory of Horticultural Plant Biology, Huazhong Agricultural University, Wuhan 430070, China
[2]College of Bioengineering, Jingchu University of Technology, Jingmen 448000, China
[3]Institute of Horticultural Sciences, Jiangxi Academy of Agricultural Sciences, Nanchang 330200, China
[4]Hubei Collaborative Innovation Center for the Characteristic Resources Exploitation of Dabie Mountains, Huanggang, Hubei 438000, China
Correspondence to: Z. Luo (E-mail: luozhr@mail.hzau.edu.cn)

ABSTRACT: Persimmon fallen leaves were employed to prepare a renewable and low-cost biosorbent named as NPFL. Effects of initial pH, contact time, initial Pb(II) concentration, coexisting metal ions, and ionic strength on adsorption of Pb(II) from aqueous solution by NPFL were studied in detail. Enhanced removal capacity of NPFL toward Pb(II) was observed, and the maximum adsorption capacity was evaluated as 256 mg g^{-1} by Langmuir modeling calculation. The fast adsorption process and the well-fitted kinetics data with pseudo-second-order model indicated that chemisorption is the main rate-limiting step for the adsorption process. NPFL had superior adsorption selectivity for Pb(II) from aqueous solution with coexisting metal ions. Characterization of NPFL and adsorption mechanism (electrostatic attraction, ion exchange, and chelation) were performed using XRD, SEM-EDS, FT-IR, XPS, and TGA. The results suggested that NPFL could be utilized as a potential candidate for the preconcentration of Pb(II) recovery and its removal in practice. © 2016 Wiley Periodicals, Inc. J. Appl. Polym. Sci. **2016**, *133*, 43656.

KEYWORDS: adsorption; biopolymers and renewable polymers; kinetics; thermogravimetric analysis; X-ray

Received 15 November 2015; accepted 20 March 2016
DOI: 10.1002/app.43656

INTRODUCTION

Heavy metal ions, the main contamination of water system, have caused serious environmental issues worldwide.[1,2] Pb, as one of the "Big Three" toxic metals,[3] has been widely applied in various industrial processes.[4,5] Rivers and lakes polluted by Pb(II)-containing wastewaters become a threat to plant and animal life because Pb(II) is a hazardous unbiodegradable element which accumulates in the food chain.[6] For the sake of clean ground- and surface-water system, industrial wastewater should be treated and standardized before discharging into the environment.[7] Various treatment techniques have been employed to eliminate Pb from aqueous solution, but some conventional methods are either low efficient or high cost.[8] Eliminating low concentration of Pb from aqueous solution is also quite difficult by these conventional methods. Since the World Health Organization (WHO) has made a specification of <0.05 mg L^{-1} in drinking water,[9] there is an urgent need to raise promising alternative approaches for purification of Pb(II)-containing wastewaters. Nowadays, adsorption has become an effective treatment process for heavy metal ions removal from micropolluted water.[10–13] Adsorbent prepared from biomaterials has been considered as ecofriendly, reusable, low-cost, and highly effective candidates for the removal of heavy metal ions.[14–19]

Besides other agricultural materials, tree leaves received huge interests by researchers lately: Ficus religiosa leaves,[20] *Hevea brasiliensis* leaves,[21] fallen *Cinnamomum camphora* leaves,[22] bael leaves,[23] *Moringa oleifera* leaves,[24] Neem leaves,[25] *Ficus hispida* leaves,[26] and *Solanum melongena* leaves[27] have been utilized for the removal of Pb. Most of the previous reports used green fresh leaves which are unfavorable for trees biologically. In this article, fallen leaves of persimmon (*Diospyros kaki* Thunb.) were first employed to prepare a new kind of biosorbent (named as NPFL) for the removal of Pb. Persimmon is a kind of deciduous fruit tree, and large amounts of its leaves regularly fall during autumn. Many pests rely on these fallen leaves for their survival during winter season, thus causing different diseases in persimmon. It is necessary to collect these leaves timely and dispose them properly. Utilization of these fallen leaves also favors

Additional Supporting Information may be found in the online version of this article.

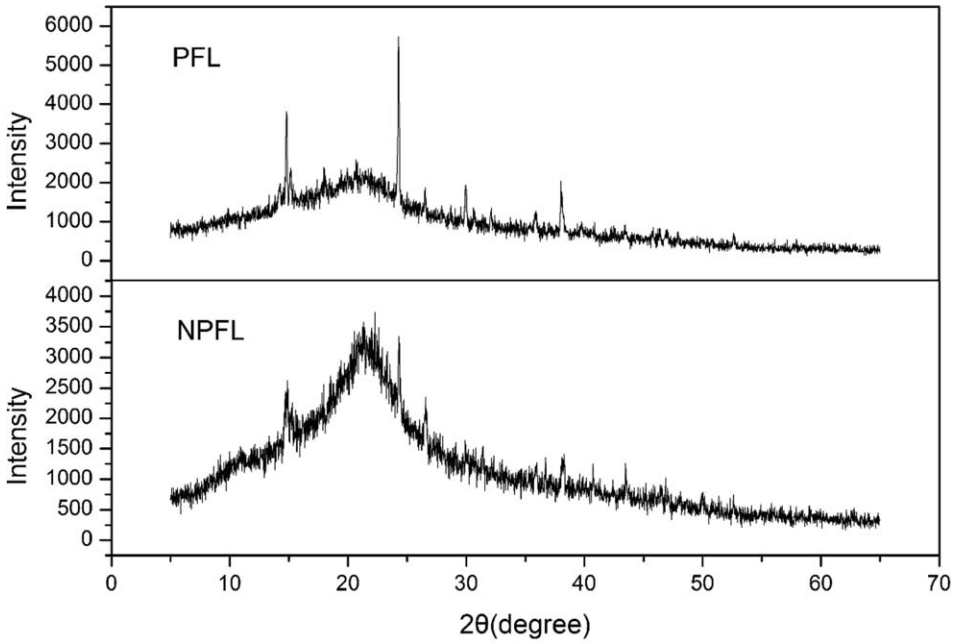

Figure 1. X-ray diffraction pattern of PFL and NPFL.

the concept of sustainable development. Moreover, compared with other kinds of fallen leaves, persimmon-fallen leaves contain the largest amount of persimmon tannin. The functional groups of persimmon tannin have high affinity for heavy metal ions.[28–33] Therefore, fallen leaves of persimmon can be a favorable raw material of adsorbents for binding heavy metal ions; however, no such related work has been reported until now.

Preparation for biosorbents should be simple and feasible to realize industrial application.[34] In this research, NPFL was prepared by treating these fallen leaves with NaOH and characterized by scanning electron microscope (SEM), X-ray diffraction (XRD), and thermal gravimetric analyzer (TGA). The adsorption behavior of NPFL toward Pb(II) was investigated in detail to study the effects of initial pH, contact time, initial Pb(II) concentration, coexisting metal ions, and ionic strength. The results revealed that after treating with NaOH, the adsorption capacity of persimmon-fallen leaves toward lead was enhanced significantly. To analyze the adsorption mechanism, SEM-EDS, FT-IR, and XPS were applied. Investigation of the potential application of NPFL was conducted in real industrial wastewater.

EXPERIMENTAL

Materials and Chemicals

$Pb(NO_3)_2$, NaOH, HNO_3, $NaNO_3$, KNO_3, $Mg(NO_3)_2{\cdot}6H_2O$, $Ca(NO_3)_2{\cdot}4H_2O$, $Ni(NO_3)_2{\cdot}6H_2O$, $Mn(NO_3)_2{\cdot}4H_2O$, and $Zn(NO_3)_2{\cdot}6H_2O$ were purchased from Sinopharm Chemical Reagent Co. Ltd., Beijing, China. A stock solution containing 1000 mg L^{-1} Pb(II) was prepared with deionized water and was subsequently diluted for a certain concentration. The pH value of the solution was adjusted using 0.1 *M* HNO_3 and/or 0.1 *M* NaOH. Deionized water was used throughout the study. All the chemicals applied in this study were of analytical reagent grade and were utilized without any purification.

Preparation of the Adsorbent

Persimmon-fallen leaves were collected locally, from Persimmon Repository of Huazhong Agricultural University, Wuhan, China. These leaves were washed with tap water to remove dirt and soluble impurities and then rinsed with deionized water. The rinsed leaves were dried in an oven at 65 °C until a constant weight, and then ground and sieved to 60 mesh. The obtained leaf powder named "PFL" was stored in a sealed dark-brown bottle for the chemical modification. The PFL was modified as following procedures: (1) 1 g of PFL was weighed and transferred to a conical flask, and 400 mL 0.25 *M* NaOH was added; (2) the obtained mixture was stirred for 3 h by magnetic stirrer at room temperature; and (3) the adsorbent was obtained by vacuum filtration and washed with deionized water repeatedly until the filtrate was clear and neutral. Afterward, it was dried in an oven at 65 °C until a constant weight. Finally, about 0.8 g NPFL was obtained and kept in a sealed dark-brown bottle for subsequent experiments.

Characterization

Zeta potentials of NPFL were measured over the pH range of 2.0–9.0 on a Zetasizer (Malvern ZEN 3600). The X-ray diffraction (XRD) patterns were recorded by using X-ray diffractometer (Bruker D8 advance). Surface morphology of NPFL and Pb(II)-loaded NPFL were examined in an SEM (JSM-5610LV) equipped with an energy dispersive X-ray spectrometer (EDS). The FT-IR spectra of NPFL and Pb(II)-loaded NPFL were measured by Thermo Nicolet Nexus spectrophotometer using KBr pellet method. The XPS spectra of NPFL, before and after adsorption, were recorded by VG Multilab 2000 instrument, and a software package of Avantage 4.54 was used to fit the O_{1s} and Pb_{1s} spectra peaks. The BET surface area of the adsorbents was measured on Quantachrome Autosorb-1, JEDL-6390 LV. The thermal gravity (TG) and differential thermal gravity (DTG) curves were obtained on a Discovery thermogravimetric

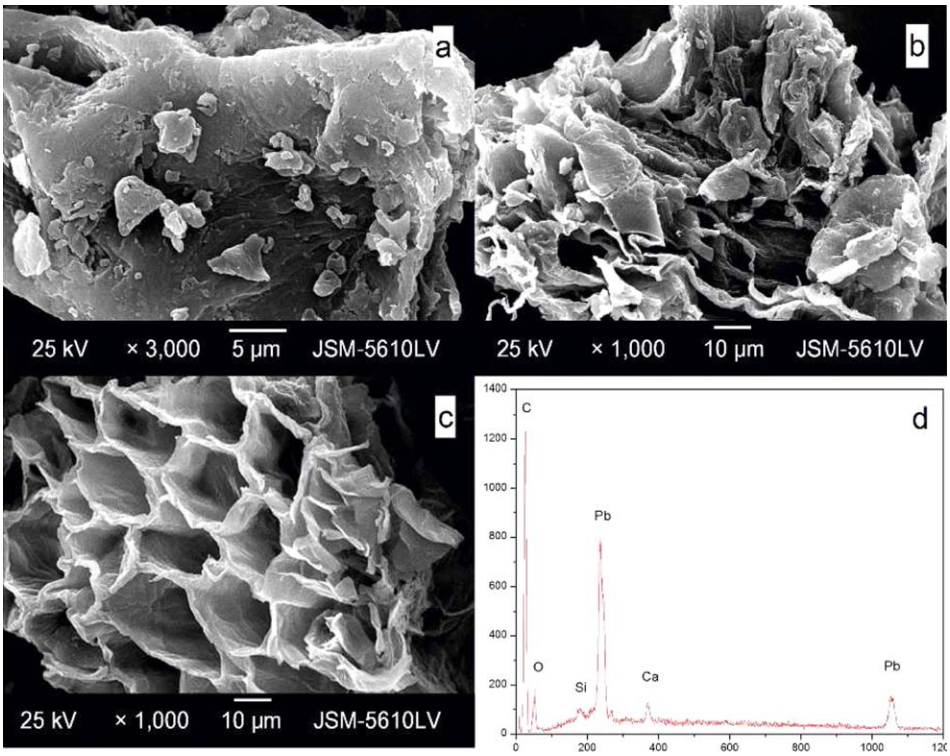

Figure 2. SEM images of (a) PFL, (b) NPFL, and (c) Pb(II)-NPFL. (d) EDS spectra of Pb(II)-loaded NPFL. [Color figure can be viewed in the online issue, which is available at wileyonlinelibrary.com.]

analyzer, on a temperature level from 25 to 800 °C with a speed of 10 °C/min under air flow.

Adsorption Experiments

Batch Adsorption Tests. A gas bath thermostat shaker (Thermo MAXQ-4000) was applied for the batch adsorption experiments. Certain concentrations of Pb(II) solution were prepared by diluting a stock solution containing 1000 mg L^{-1} Pb(II). The pH of the solution was adjusted using 0.1 mol L^{-1} HNO_3 and/or NaOH by a pH meter (UB-7, Sartorius) to a desired value. The adsorbent dosage of 0.2 g L^{-1} was employed. For instance, in a typical batch adsorption experiment, 10 mg NPFL and 50 mL Pb(II) solution were mixed in sealed conical flasks and shaken together at 30 °C for 24 h at a speed of 200 rpm. A blank experiment of 50 mL Pb(II) solution with no NPFL was also carried out simultaneously. The mixture was separated by filtration and the filtrate was collected for analysis by atomic absorption spectrophotometer (AAS, Varian Spectra AA 220; Shimazu 6300C). The adsorption capacity (q_e) was calculated through the following equation:

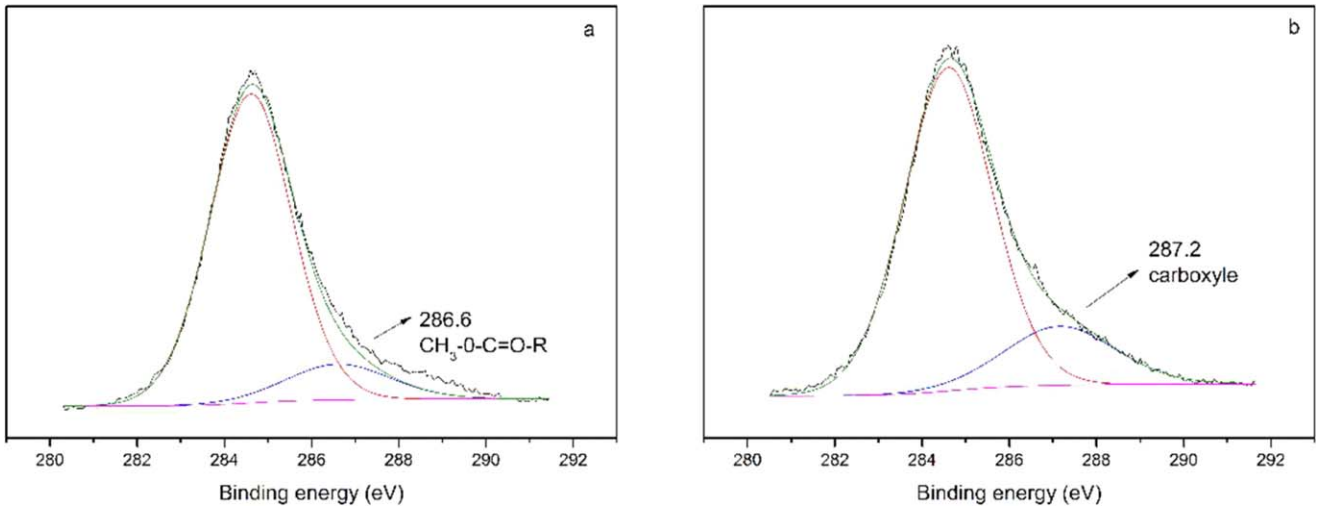

Figure 3. XPS C1s spectra of persimmon fallen leaves (a) before and (b) after treated with NaOH. [Color figure can be viewed in the online issue, which is available at wileyonlinelibrary.com.]

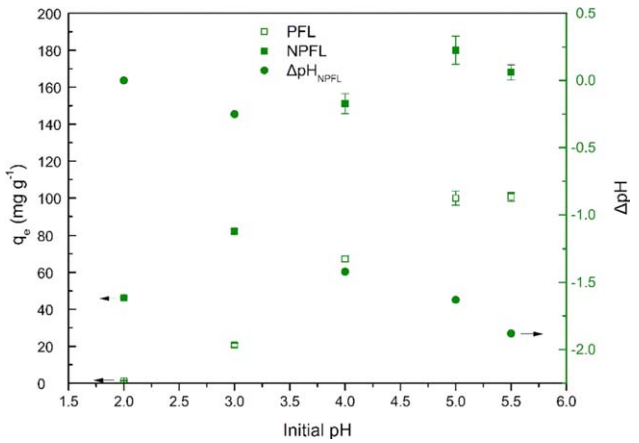

Figure 4. Effect of initial pH on Pb(II) adsorption onto PFL and NPFL and the pH changes after adsorption by NPFL (q_e: adsorption capacity). Weight of adsorbent = 10 mg; volume of Pb(II) solution = 50 mL; initial concentration of Pb(II) = 50 mg L^{-1}; temperature = 30 °C; shaking time = 24 h; shaking speed = 200 rpm. [Color figure can be viewed in the online issue, which is available at wileyonlinelibrary.com.]

$$q_e = \frac{(C_i - C_e)V}{m} \quad (1)$$

where, C_i (mg L^{-1}) and C_e (mg L^{-1}) are initial and equilibrium concentrations of Pb(II) in solution, respectively; m (g) is the weight of NPFL; and V (L) is the volume of Pb(II) solution. Every single experiment was repeated three times, and the mean values of the results with standard deviation were presented in the figures.

To examine the effect of pH, 50 mg L^{-1} of Pb(II) solution was adjusted to pH values ranged from 2.0 to 5.5. Adsorption isotherm was obtained at 30 °C with different initial Pb(II) concentration (50–100 mg L^{-1}). For kinetics study, 50 mg L^{-1} of Pb(II) solution was reacted with NPFL for varied time (5–480 min). The selectivity of NPFL toward Pb(II) was performed in binary metal ions systems of Pb(II) & Na(I), Pb(II) & K(I), Pb(II) & Mg(II), Pb(II) & Ca(II), Pb(II) & Ni(II), Pb(II) & Mn(II), Pb(II) & Zn(II), and Pb(II) & Cu(II). As for the ionic strength test, ionic strengths of 2.2–87 mol L^{-1} Na^+ were adopted.

Column Adsorption and Desorption Tests. A glass column of 20 cm length (1 cm of inner diameter) was used to conduct the column adsorption and desorption experiments. The upper part of the column was connected with a constant flow pump (DHL-A) to keep the fixed flow rates. The effluent solution from the column was collected by the automatic fraction collector (BSZ-100) hourly for further analysis. The operation of column adsorption test was identical to our previous report[35] with some minor changes. First, 300 mg NPFL was added into the glass column slowly with a plastic dropper by the method of wet filling. Second, the packed column was conditioned by passing deionized water for 24 h. Third, 50 mg L^{-1} of Pb(II) solution was pumped through the column at a constant rate of 3.0 mL h^{-1} by the peristaltic pump. The effluent solution from the column was collected by the automatic fraction collector hourly for further analysis. After the breakthrough of Pb(II) was obtained, the NPFL column was washed with deionized water for 24 h and the effluent was analyzed to guarantee that no Pb(II) ion was existed in the column. The Pb(II)-loaded NPFL was regenerated with 0.3 *M* of HCl at the same flow rate. The bed volume (*B.V.*) of the effluent is defined as

$$B.V. = \frac{v.t}{V} \quad (2)$$

Where v, t, and V are the flow rate of the solution, the time for which the feed solution was pumped through the bed, and the wet volume of the packed adsorbent, respectively.

RESULTS AND DISCUSSION

Characterization

Persimmon leaves comprised biological macromolecules and polymers like cellulose, lignin, persimmon tannin, flavonone glycosides, polysaccharide, and so on, thus it is rather difficult to elaborately characterize the adsorbent derived from fallen leaves of persimmon. In this study, a one-step simple and facile method was employed to prepare the renewable and low-cost adsorbent by treating persimmon leaves with diluted NaOH, and then XRD, SEM, and XPS analyses were carried out to reveal the different characteristics between PFL and NPFL.

As can be seen from Figure 1, the peaks of PFL at 2θ value of 14.8°, 24.3°, and 38.0° indicated the existence of calcium oxalate hydrate,[36] while after modification, the intensity of these peaks decreased dramatically and became broader. It indicated that no crystallinity is observed in NPFL which favors for metal ions binding in the surface of the adsorbent.[37]

The SEM images of PFL and NPFL are shown in Figure 2(a,b), and after treated with NaOH, the persimmon-fallen leaves showed different surface morphology. Alkali activation has also

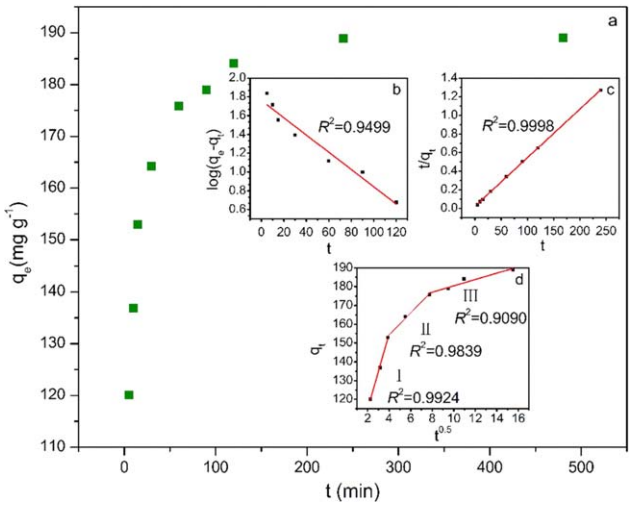

Figure 5. (a) Effect of contact time on adsorption; models fit of kinetic data: (b) pseudo-first-order, (c) pseudo-second-order, and (d) intraparticle diffusion plots (q_t: adsorption capacity at time t, mg g^{-1}; q_e: adsorption capacity at equilibrium, mg g^{-1}). Weight of adsorbent = 10 mg; volume of Pb(II) solution = 50 mL; pH = 5; temperature = 30 °C; shaking speed = 200 rpm. [Color figure can be viewed in the online issue, which is available at wileyonlinelibrary.com.]

Table I. Pseudo-First-Order and Pseudo-Second-Order Parameters for Pb(II) Adsorption on NPFL

Experimental	Pseudo-first-order			Pseudo-second-order		
q_e (mg g^{-1})	$K_1 \times 10^{-2}$ (min^{-1})	R^2	$q_{e,cal}$ (mg g^{-1})	$K_2 \times 10^{-3}$ (g mg^{-1} min^{-1})	R^2	$q_{e,cal}$ (mg g^{-1})
189.00	2.12	0.9499	57.81	1.17	0.9998	192.31

Table II. Intraparticle Diffusion Parameters for Pb(II) Adsorption on NPFL

Phase I			Phase II			Phase III		
K_{id1} (mg g^{-1} $min^{-0.5}$)	R^2	C	K_{id2} (mg g^{-1} $min^{-0.5}$)	R^2	C	K_{id3} (mg g^{-1} $min^{-0.5}$)	R^2	C
20.00	0.9924	74.81	5.85	0.9839	130.99	1.69	0.9090	163.50

been widely used on various carbon materials[38] and tannin-based hydrogels[39] to increase the surface area. It is reported that tannin–formaldehyde hydrogels activated by alkali produced homogeneous materials with a foam-like structure presenting high surface areas and micropore volumes even when very low hydroxide amounts were used.[39] After treating with diluted NaOH, many gaps and fractures appeared on the surface of NPFL which made the generated material wrinkled [Figure 2(b)], providing more active sites for metal ions binding. Treatment with NaOH also promoted the conversion of methyl esters which inhibit the adsorption to carboxylate ligands.[40] XPS C1s spectra of PFL and NPFL were illustrated in Figure 3. It is clear that after treating with NaOH, the peak at 286.6 eV which stands for methyl ester is transferred to 287.2 eV which represents carboxylate.

Parameters Affecting the Adsorption Process

Effect of pH. Figure 4 illustrates the amount of Pb(II) adsorbed by raw and enhanced materials and the variation in pH after adsorption of Pb(II) by NPFL. The ΔpH was calculated by the equilibrium pH of the solution after adsorption minus the equilibrium pH of blank solution with equal amount of deionized water and NPFL. The pH of the blank solution increased after the addition of NPFL due to the buffer action of the functional groups on the adsorbent. The negative values of ΔpH may be caused by the release of H^+ from the functional groups of NPFL when Pb^{2+} was exchanged with H^+ during adsorption.

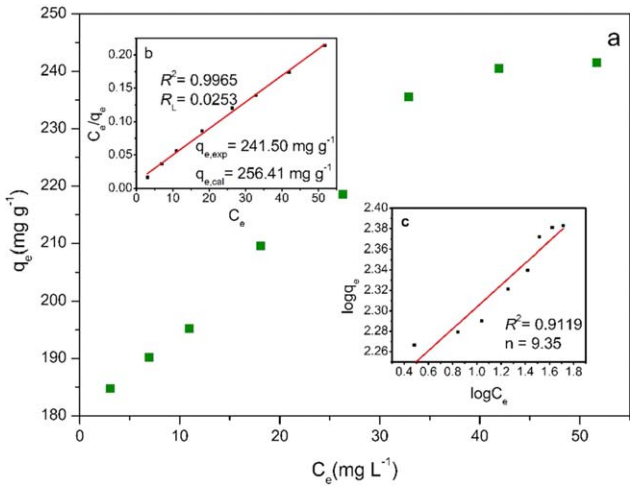

Figure 6. (a) Effect of initial concentration on Pb(II) adsorption; (b) Langmuir and (c) Freundlich plots (C_e: equilibrium concentration, mg L^{-1}; q_e: adsorption capacity at equilibrium, mg g^{-1}). Weight of adsorbent = 10 mg; volume of Pb(II) solution = 50 mL; pH = 5; shaking speed = 200 rpm. [Color figure can be viewed in the online issue, which is available at wileyonlinelibrary.com.]

The maximum adsorption capacity of NPFL observed at pH 5 was 80.2% higher than that displayed by the raw material at the same pH value. Since both the chemical speciation of the heavy metal ions in the aqueous solution and the charge and the active sites on the surface of the adsorbent are influenced by the pH, adsorption of Pb(II) is strongly dependent on the initial pH of the aqueous solution.[41] At pH values below 3, Pb(II) was not adsorbed efficiently by NPFL from aqueous solutions. The adsorption capacity of NPFL increased rapidly as the pH of the solution was increased from 3 to 5. The highest adsorption capacity of 180 mg g^{-1} was observed at pH 5. This pH-dependent nature of Pb(II) adsorption could be rationalized based on the zeta potential of NPFL (Supporting Information, Figure S1). From Supporting Information, Figure S2, it is evident that in the pH range 2–6, Pb(II) predominantly existed as the Pb^{2+} species based on equilibrium calculations when the concentration of Pb(II) was 50 mg L^{-1}. NPFL displayed the zero charge potential at pH 3.3. Therefore, when the pH of the solution was lower than 3.3, positive charges at the active sites on the surface of NPFL would hinder the adsorption of Pb^{2+} because of electrostatic repulsion between Pb(II) and NPFL and exhibited that only minute quantities of Pb(II) ions were adsorbed.[42] Thus, electrostatic attraction between the negatively charged NPFL and Pb^{2+} promoted the adsorption uptake when the solution pH was increased from 3 to 5. The adsorption capacity decreased a little at pH 5.5. Hence, adjusting the solution pH to 5 would promote the Pb(II) adsorption. Therefore, all the following tests were conducted at pH 5 unless it was specified.

Effect of Reaction Time. To explore the equilibrium time for maximum uptake, adsorption of Pb(II) onto NPFL was carried out under varied contact time (5–480 min) and the results are shown in Figure 5(a). It is obvious that Pb(II) adsorption occurred quickly at the first 60 min and then increased gradually with increasing the contact time from 60 to 480 min. The maximum adsorption capacity was obtained at 240 min.

Table III. Langmuir and Freundlich Parameters for Pb(II) Adsorption on NPFL

Experimental	Langmuir			Freundlich		
Q_e (mg g^{-1})	Q_m (mg g^{-1})	K_L (L mg^{-1})	R^2	K_F ($mg^{1-1/n}$ $L^{1/n}$ g^{-1})	1/n	R^2
242	256	0.39	0.9965	9.0	9.35	0.9119

To further study the adsorption kinetics and determine the rate-limiting step of Pb(II) onto NPFL, the experimental data were fitted with pseudo-first-order, pseudo-second-order, mass transfer, and intraparticle diffusion models (linear equations are shown in Supporting Information, Table S1). Kinetics constants and correlation coefficient (R^2) of these models are calculated from the experimental plot in Figure 5(a) and the values are shown in Table I. The correlation coefficient of pseudo-second-order model was above 0.99, surpassing that of pseudo-first-order model. Moreover, the calculated q_e (the adsorption capacity at equilibrium) values were closer to the experimental data. Pb(II) adsorption onto NPFL could be best described by the pseudo-second-order model, which revealed that chemisorption might be the rate-limiting step for adsorption between Pb(II) and NPFL with no mass transfer involved in solution.[43] It was further proved by plotting $\ln[(Ct/C_0) - 1/(1 + mK)]$ versus t in Supporting Information, Figure S3, where a linear graphical relation was not obtained ($R^2 = 0.5860$). Pseudo-second-order model is also based on the assumption that the rate-controlling step is the surface adsorption by valence forces through sharing or exchanging of electrons between adsorbent and adsorbate.[44]

The multilinear plots in Figure 5(d) demonstrated that there are three phases influencing the adsorption process. For each phase, the rate constant and the correlation coefficient are listed in Table II. It is observed that the order of adsorption rate constants was $K_{id1} > K_{id2} > K_{id3}$. In the first sharp stage where the K_{id1} was the largest, Pb(II) was adsorbed by the exterior surface of NPFL.[44] High initial Pb(II) concentration might be the driving force for diffusion. This process completed in 15 min, which was a little longer than reported in other studies.[45] The second phase where the K_{id2} was medium was a gradual uptake, which revealed the intraparticle diffusion as the rate-limiting step.[24,27,46] The final phase was the equilibrium stage, where the K_{id3} was lower than the other two phases generated by low lead concentration left in the solution and the reduction of active binding sites present on NPFL. It could be seen that the lines did not go through the origin, which signified the rate was controlled by not only the intraparticle diffusion but also some other mechanisms, such as boundary layer control.[47]

Effect of Initial Lead Concentration. It can be seen from Figure 6(a) that the adsorption capacity for Pb(II) removal increased with increasing of the equilibrium Pb(II) concentration by changing the initial Pb(II) concentration from 40 to 100 mg L^{-1}. To explore the Pb(II) adsorption behavior in terms of the adsorption capability of NPFL and the detailed adsorption process, isotherms such as Langmuir and Freundlich (linear equations in Supporting Information, Table S1) were used to model the equilibrium data. And Table III presented the equilibrium constants and correlation coefficients (R^2) of these models calculated from experimental plot in Figure 6(a).

The Langmuir equation is a well-known typical model for isotherm data fitting. It is based on the monolayer adsorption of metal ions on the surface of adsorbents. It can be seen from Figure 6(b) that Langmuir fitted well with the experimental data according to the high correlation coefficients ($R^2 > 0.99$). The constants of isotherm can predict whether an adsorption system is favorable or not. The essential features of the Langmuir isotherm can be expressed in terms of a dimensionless constant separation factor (R_L), which is defined as

$$R_L = \frac{1}{1 + K_L c_i} \tag{3}$$

where K_L is the Langmuir constant (L mg^{-1}) and c_i is the highest initial metal concentration (mg L^{-1}). The value of R_L indicates the types of isotherm to be among unfavorable ($R_L > 1$), linear ($R_L = 1$), favorable ($0 < R_L < 1$), or irreversible ($R_L = 0$).[22]

Table IV. A Comparative Study of Adsorption Parameters for Pb(II) Onto Leaf-Based Adsorbents

Leaves biosorbent	Maximum capacity (mg g^{-1})	Optimal pH	Kinetics	Isotherm	Reference
NPFL	256	5	Pseudo-2nd order	Langmuir	Present study
Moringa oleifera leaves	209.54	4-6	Pseudo-2nd order	Langmuir	24
Bael leaves	104	5.1	Pseudo-2nd order	Langmuir	23
Hevea brasiliensis leaves	95.3	4-5	Pseudo-2nd order	Langmuir	21
Neem leaves	91.34	5	Pseudo-2nd order	Langmuir	25
Fallen *Cinnamomum camphora* leaves	75.82	5	Pseudo-2nd order	Langmuir	22
Solanum melongena leaves	71.42	5	Pseudo-2nd order	Langmuir	27
Ficus religiosa leaves	37.45	4	Pseudo-2nd order	Langmuir	20
Ficus hispida leaves	32.42	6.1	Pseudo-2nd order	Langmuir	26

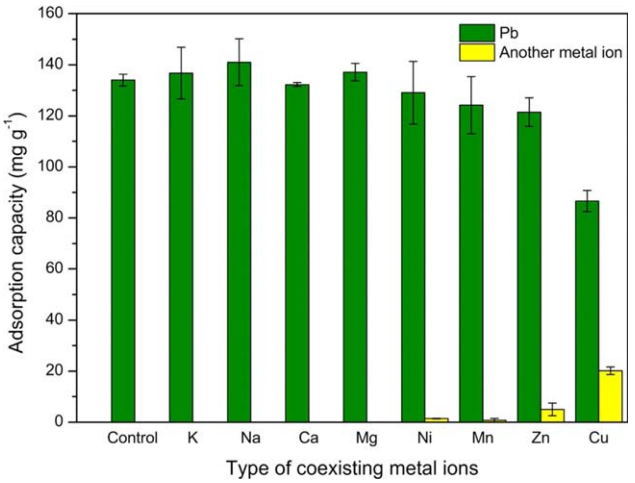

Figure 7. The interfaces of coexisting metal ions on Pb(II) adsorption in binary ion system. Weight of adsorbent = 10 mg; volume of Pb(II) solution = 50 mL; initial concentration of metal ions = 0.25 mol L^{-1}; temperature = 30 °C; shaking time = 24 h; shaking speed = 200 rpm. [Color figure can be viewed in the online issue, which is available at wileyonlinelibrary.com.]

The calculated value of R_L was 0.0253, which meant favorable adsorption process.

The Freundlich isotherm, as an empirical relationship, assumed that the adsorption occurs on a heterogeneous surface. The favorability of adsorption can also be revealed by n value of Freundlich modelling. Generally, *n* in the range of 2–10 represent good, 1–2 moderately difficult, and <1 poor adsorption behaviors.[22] As can be seen from Table III, the value of *n* is 9.35, also indicating adsorption between NPFL and Pb(II) is favorable.

The maximum monolayer adsorption capacity was calculated as 256 mg g^{-1} at 30 °C. Table IV showed the maximum capacity of Pb(II) adsorption by different kinds of leaf-based adsorbents. Compared with other adsorbents, NPFL, as a sorbent prepared from persimmon-fallen leaves, exhibited good potential for Pb(II) removal from aqueous solutions.

Effect of Coexisting Metal Ions and Ionic Strength. In practical applications, the wastewaters generally contain various kinds of metal ions, and some coexisting metal ions may affect Pb(II) adsorption. Thus, it is important to assess the effect of co-ions for enhancing the application at industrial scales.[48] The adsorption of Pb(II) in presence of coexisting cations (K^+, Na^+, Ca^{2+}, Mg^{2+}, Mn^{2+}, Ni^{2+}, and Zn^{2+}) was evaluated in binary metal ion systems. The results in Figure 7 indicated good selectivity of NPFL toward Pb(II). Comparing adsorption capacity of Pb(II) in the control sample with that in the binary metal groups, interference of coexisting cations had no noticeable effect on adsorption of Pb(II) except that of Pb(II) & Cu(II) group. To compare the adsorption capacity better, we convert the unit to mmol g^{-1}, and the loading amount for Pb(II) and Cu(II) was 0.42 and 0.32 mmol g^{-1}, respectively. The decrease of Pb(II) adsorption capacity might attribute to the adsorption competition between Cu(II) and Pb^{2+}, thereby disabling NPFL to interact with the positively charged adsorbate.[49] The decrease of Pb(II) uptake in Supporting Information, Figure S4 with the increase of ionic strength further confirmed this phenomenon.

Adsorption Mechanism

In Figure 2(d), the appearance of Pb(II) characteristic peaks after adsorption confirmed the presence of Pb(II) on NPFL. The SEM images of NPFL before and after adsorption in Figure 2(b,c), respectively, were slightly different indicating that the adsorption process or Pb(II) capture would change the morphology of NPFL to some extent. FT-IR spectra shown in Supporting Information, Figure S5, illustrated that the functional groups changed before and after adsorption. Band positions of the function groups are demonstrated in Supporting Information, Table S2. From the disappearance of C–O stretching, it was regarded as the interaction between Pb(II) and O atom.

XPS was conducted to further confirm the interaction between Pb(II) and O of the functional groups on NPFL. XPS O_{1s} and Pb_{4f} spectra of Pb(II)–NPFL are illustrated in Figure 8. After adsorption of Pb(II), the peak of Pb_{4f} at 138.85 eV implied the bonding between lead ions and carboxyl group of NPFL.[50] The peak at 143.65 eV further confirmed the fixation of Pb onto the NPFL.[51] The peak of O_{1s} at 530.70 eV also proved the appearance of PbO after adsorption coinciding with the above results. The ion exchange between H^+ and Pb^{2+} was verified by measuring the equilibrium pH of the solution after adsorption. The

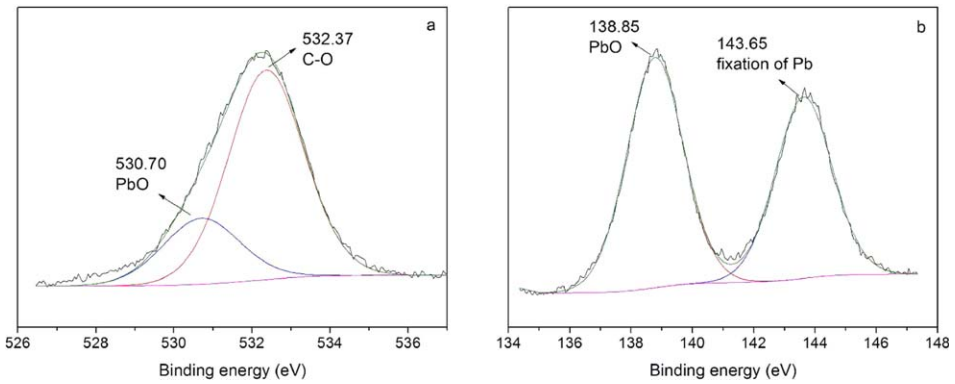

Figure 8. XPS spectra of (a) O_{1s} and (b) Pb_{4f} of NPFL after adsorption of Pb(II). [Color figure can be viewed in the online issue, which is available at wileyonlinelibrary.com.]

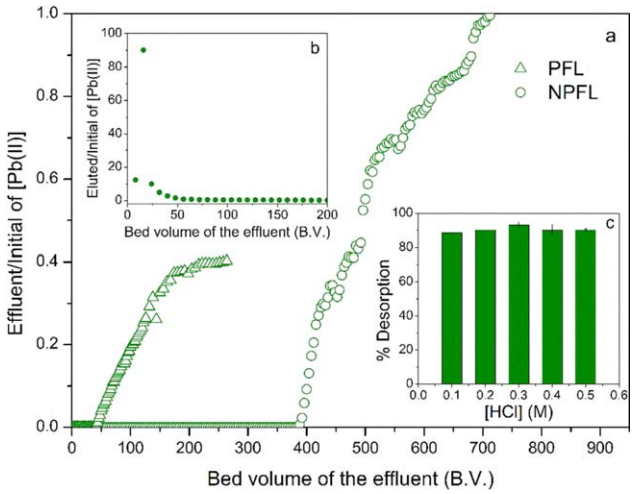

Figure 9. (a) Breakthrough and (b) elution profiles of Pb(II) on NPFL; (c) desorption of Pb(II)-NPFL using diluted HCl solution (C_e: equilibrium concentration of Pb(II); C_i: initial concentration of Pb(II); C_t: concentration of Pb(II) in the effluent). Weight of adsorbent = 300 mg; initial concentration of Pb(II) = 50 mg L^{-1}; flow rate = 3 mL h^{-1}; concentrations of HCl = 0.1–0.5 mol L^{-1}. [Color figure can be viewed in the online issue, which is available at wileyonlinelibrary.com.]

values of ΔpH in different initial pH are shown in Figure 4. The release of H^+ accounts for the negative values of ΔpH.

As illustrated in Table IV, the adsorption capacity of NPFL had a significant advantage over other existing leaf-based adsorbents. As shown in Figure 2, after modification with NaOH, the appearance of NPFL became wrinkled which means it may have larger surface area and provide more active sites for Pb(II) binding. The BET measurement was also conducted to evaluate the exact improvement in surface area. The BET surface area of the adsorbent increased from 0.948 to 6.63 cm^2 g^{-1}. What is more, persimmon tannin which NPFL contains can effectively improve the adsorption capacity. Moreover, the zero charge potential of NPFL was calculated at pH 3.3. When the solution pH was above that, the surface charge of NPFL would be negative which promoted the Pb^{2+} adsorption on NPFL due to electrostatic attraction. The proposed mechanism could be summarized as (1) the electrostatic attraction between negatively charged active sites on NPFL and Pb^{2+}; (2) the ionic exchange between H^+ of phenol hydroxyl group and Pb^{2+}; (3) the chelation between hydroxyl group and carboxylate ligand on NPFL and Pb^{2+} with the formation of Pb(II) complex.

Fixed-Bed Column Adsorption and Desorption

As seen in Figure 9(a), Pb(II) breaks through the PFL column quickly, and the effective treatment volume is only 48 mL (40 B.V.). In contrast, the effective treatment volume of NPFL is as high as 460.8 mL (384 B.V.) under the identical conditions, which is nearly 8.6 times higher than that of the PFL. Compared with PFL, NPFL has showed significant enhancement for lead removal not only in batch tests but also in continuous adsorption. The regeneration of NPFL was conducted using 0.1–0.5 *M* HCl, and 0.3 *M* HCl was chosen as the optimal desorption reagent [Figure 9(c)]. As presented in Figure 9(b), Pb(II) was eluted quickly with a concentration factor of 90.2. The high degree of enrichment enabled NPFL as a good candidate for industrial application in preconcentration of Pb(II)-containing wastewater. The result of reusability test shown in Supporting Information, Table S3 indicates that NPFL can be used for at least 5 times even though the adsorption capacity decreases slightly.

Application in industrial Wastewater

To explore the potential application of NPFL in practical wastewater, a sample of industrial wastewater was kindly provided by GEM high-tech Co. Ltd., China. The result of water analysis of the industrial wastewater before and after treatment with NPFL is shown in Table V. After treating with NPFL (10 g L^{-1}), the concentrations of Pb(II), Zn(II), and Ni(II) in the wastewater declined significantly. Concentration of Pb(II) declined from 4.73 to 0.87 mg L^{-1}, with 81.61% removal efficiency; the removal ratio of Zn(II) was 95.95% and that of Ni(II) was 87.91%. The pH value was 6.66 after treating with NPFL. Other metals such as Na, K, and Mg in the wastewater showed little competition with heavy metals, which could be confirmed by the result that the concentrations of Na^+, K^+, and Mg^{2+} changed little before and after treatment even concentration of Na^+ was as high as 3675 mg L^{-1}. These results demonstrated that NPFL could effectively treat practical wastewater containing heavy metals.

Recovery of Pb(II) by Incineration

After adsorption, Pb(II) can also be recovered by means of the incineration. Figure 10 shows the TG and DTG curves of NPFL before and after adsorption of Pb(II). The significant weight loss of NPFL and Pb-loaded NPFL was observed in TG curves. From the TGA curve of NPFL, it was found that NPFL began to decompose at 200 °C with the inflection point at 313 °C and ceased losing weight at 477 °C. The TGA curve of Pb-loaded NPFL was similar to that of NPFL with these three points at 200, 300, and 451 °C which were slightly lower than that of NPFL. The high decomposition temperature revealed that NPFL is of excellent thermal stability. The organic part of NPFL and Pb-loaded NPFL was mainly decomposed to CO_2 and H_2O with minor amount of NO_2 and SO_2, whereas the inorganic part might be turned into oxide form with the weight percentage of 13.72% and 20.23% of NPFL and Pb-loaded NPFL, respectively. After incineration, the ash obtained is rich in Pb(II), which can be recycled as a secondary lead resource or disposed properly.

Table V. Quality Analysis of Industrial Wastewater from GEM Treated by NPFL

	Pb	Na	K	Mg	Zn	Ni	pH
Before treatment (mg L^{-1})	4.73	3674.86	5.09	11.84	16.56	8.23	5
After treatment (mg L^{-1})	0.87	3652.19	5.02	11.26	0.67	0.995	6.66
Removal ratio (%)	81.61	-	-	-	95.95	87.91	-

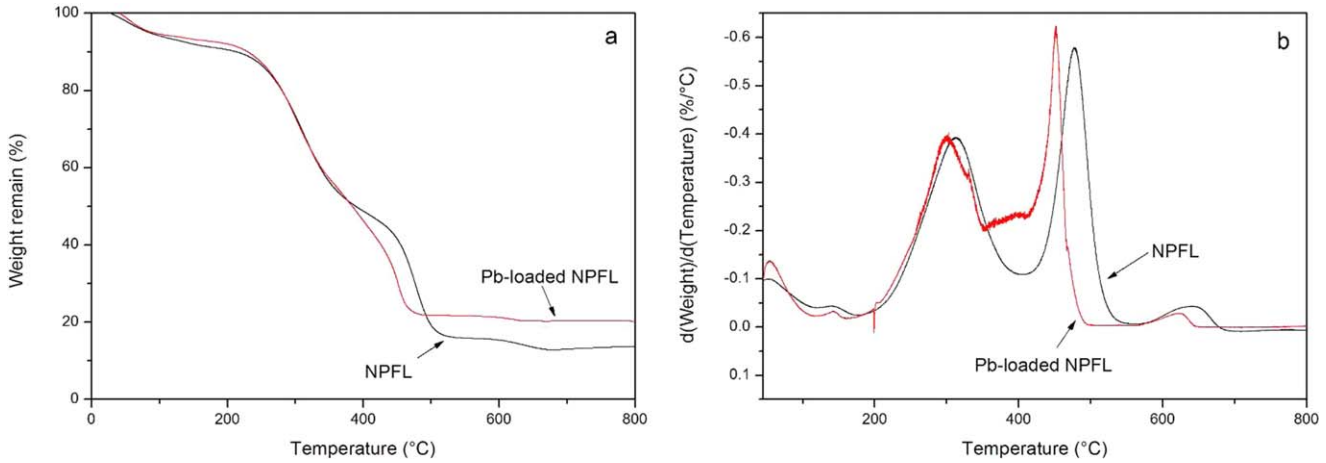

Figure 10. (a) TG and (b) DTG curves of NPFL- and Pb(II)-loaded NPFL. [Color figure can be viewed in the online issue, which is available at wileyonlinelibrary.com.]

CONCLUSIONS

The fallen leaves of persimmon tree need to be collected and treated properly to provide a clean and comfortable environment for the tree growth; however, persimmon leaves comprised many biomacromolecules like cellulose, lignin, persimmon tannin, flavonone glycosides, polysaccharide, and so on. The existing functional groups such as hydroxyl, carboxyl, phenolic, and amino in persimmon leaves have affinity for heavy metal ions. Under this premise, these fallen leaves were employed as raw material to prepare a functional adsorbent named as NPFL. This novel adsorbent exhibited enhanced removal efficiency toward Pb(II) in both the static and dynamic adsorption tests (elevated 80.2% and 860%, respectively). The maximum monolayer adsorption capacity of NPFL (256 mg g^{-1}) is the highest among the existing leaf-based adsorbents. Electrostatic attraction, ionic exchange, and chelation between functional groups on NPFL and Pb^{2+} were characterized by measuring zeta potential and ΔpH, conducting SEM-EDS, FTIR, and XPS. Substantial Pb(II) were removed by NPFL from aqueous solution of high ionic strength. NPFL can be used for at least 5 times regenerated by 0.3 *M* HCl. Moreover, in actual wastewater treatment experiments, after treating with NPFL, not only Pb(II) but also Zn(II) and Ni(II) have been removed. This study demonstrates that NPFL could be a promising candidate for the efficient treatment of industrial wastewater.

ACKNOWLEDGMENTS

This research was funded by Special Fund for Agro-scientific Research in the Public Interest (201203047) and China Scholarship Council (No. 201506760019). And the authors also appreciate the kind support of GEM high-tech Co. Ltd., China.

REFERENCES

1. Huang, G.; Wang, D.; Ma, S.; Chen, J.; Jiang, L.; Wang, P. *J. Colloid. Interface Sci.* **2015**, *445*, 294.
2. Tong, L.; Chen, J.; Yuan, Y.; Cui, Z.; Ran, M.; Zhang, Q.; Bu, J.; Yang, F.; Su, X.; Xu, H. *J. Appl. Polym. Sci.* **2015**, *132*, 132.
3. Volesky, B. *Water Res.* **2007**, *41*, 4017.
4. Sarada, B.; Prasad, M. K.; Kumar, K. K.; Murthy, C. V. *Environ. Sci. Pollut. Res. Int.* **2014**, *21*, 1314.
5. Akar, T.; Tunali, S.; Kiran, I. *Biochem. Eng. J.* **2005**, *25*, 227.
6. Sarı, A.; Tuzen, M.; Uluözlü, ÖD.; Soylak, M. *Biochem. Eng. J.* **2007**, *37*, 151.
7. Madadrang, C. J.; Kim, H. Y.; Gao, G.; Wang, N.; Zhu, J.; Feng, H.; Gorring, M.; Kasner, M. L.; Hou, S. *ACS Appl. Mater. Inter.* **2012**, *4*, 1186.
8. Li, Q.; Su, H.; Li, J.; Tan, T. *Process Biochem.* **2007**, *42*, 379.
9. Peng, X.; Xu, F.; Zhang, W.; Wang, J.; Zeng, C.; Niu, M.; Chmielewská, E. *Colloids Surf. A* **2014**, *443*, 27.
10. Li, W.; Gong, X.; Li, X.; Zhang, D.; Gong, H. *Bioresour. Technol.* **2012**, *113*, 106.
11. Mao, N.; Yang, L.; Zhao, G.; Li, X.; Li, Y. *Chem. Eng. J.* **2012**, *200-202*, 480.
12. Wu, X.; Wang, D.; Zhang, S.; Cai, W.; Yin, Y. *J. Appl. Polym. Sci.* **2015**, *132*.
13. Ahmetli, G.; Yel, E.; Deveci, H.; Bravo, Y.; Bravo, Z. *J. Appl. Polym. Sci.* **2012**, *125*, 716.
14. Anwar, J.; Shafique, U.; Waheed uz, Z.; Salman, M.; Dar, A.; Anwar, S. *Bioresour. Technol.* **2010**, *101*, 1.
15. Tan, G.; Xiao, D. *J. Hazard. Mater.* **2009**, *164*, 1359.
16. Davis, T. A.; Volesky, B.; Mucci, A. *Water Res.* **2003**, *37*, 4311.
17. Maruyama, T.; Terashima, Y.; Takeda, S.; Okazaki, F.; Goto, M. *Process Biochem.* **2014**, *49*, 850.
18. Liu, W.; Liu, Y.; Tao, Y.; Yu, Y.; Jiang, H.; Lian, H. *Environ. Sci. Pollut. Res. Int.* **2014**, *21*, 2054.
19. Zhang, B.; Fan, R.; Bai, Z.; Wang, S.; Wang, L.; Shi, J. *Environ. Sci. Pollut. Res. Int.* **2012**, *20*, 1367.
20. Qaiser, S.; Saleemi, A. R.; Umar, M. *J. Hazard. Mater.* **2009**, *166*, 998.
21. Kamal, M. H. M. A.; Azira, W. M. K. W. K.; Kasmawati, M.; Haslizaidi, Z.; Saime, W. N. W. *J. Environ. Sci. China* **2010**, *22*, 248.

22. Chen, H.; Zhao, J.; Dai, G.; Wu, J.; Yan, H. *Desalination* **2010**, *262*, 174.
23. Chakravarty, S.; Mohanty, A.; Sudha, T. N.; Upadhyay, A. K.; Konar, J.; Sircar, J. K.; Madhukar, A.; Gupta, K. K. *J. Hazard. Mater.* **2010**, *173*, 502.
24. Reddy, D. H. K.; Harinath, Y.; Seshaiah, K.; Reddy, A. V. R. *Chem. Eng. J.* **2010**, *162*, 626.
25. Zafar, M. N.; Parveen, A.; Nadeem, R. *Desalin. Water Treat.* **2013**, *51*, 4459.
26. Namdeti, R.; Pulipati, K. *Desalin. Water Treat.* **2013**, *52*, 339.
27. Yuvaraja, G.; Krishnaiah, N.; Subbaiah, M. V.; Krishnaiah, A. *Colloids Surf. B* **2014**, *114*, 75.
28. Inoue, K.; Paudyal, H.; Nakagawa, H.; Kawakita, H.; Ohto, K. *Hydrometallurgy* **2010**, *104*, 123.
29. Li, W.; Tang, Y.; Zeng, Y.; Tong, Z.; Liang, D.; Cui, W. *Chem. Eng. J.* **2012**, *193-194*, 88.
30. Nakajima, A.; Baba, Y. *Water Res.* **2004**, *38*, 2859.
31. Wang, Y.; Wang, F.; Wan, T.; Cheng, S.; Xu, G.; Cao, R.; Gao, M. *J. Wuhan Univ. Technol.* **2013**, *28*, 650.
32. Özacar, M.; Şengil, İ. A.; Türkmenler, H. *Chem. Eng. J.* **2008**, *143*, 32.
33. Zhou, Z.; Liu, F.; Huang, Y.; Wang, Z.; Li, G. *Int. J. Biol. Macromol.* **2015**, *77*, 336.
34. Pavan, F. A.; Mazzocato, A. C.; Jacques, R. A.; Dias, S. L. P. *Biochem. Eng. J.* **2008**, *40*, 357.
35. Fan, R.; Xie, F.; Guan, X.; Zhang, Q.; Luo, Z. *Bioresour. Technol.* **2014**, *163*, 167.
36. Tang, Q.; Tang, X.; Hu, M.; Li, Z.; Chen, Y.; Lou, P. *J. Hazard. Mater.* **2010**, *179*, 95.
37. Reddy, D. H. K.; Seshaiah, K.; Reddy, A. V. R.; Lee, S. M. *Carbohyd. Polym.* **2012**, *88*, 1077.
38. Wang, R.; Wang, P.; Yan, X.; Lang, J.; Peng, C.; Xue, Q. *ACS Appl. Mater. Inter.* **2012**, *4*, 5800.
39. Szczurek, A.; Amaral-Labat, G.; Fierro, V.; Pizzi, A.; Celzard, A. *Microporous Mesoporous Mater.* **2014**, *196*, 8.
40. Mosa, A. A.; El-Ghamry, A.; Trüby, P. *Water Air Soil Pollut.* **2010**, *217*, 637.
41. Hu, Q.; Paudyal, H.; Zhao, J.; Huo, F.; Inoue, K.; Liu, H. *Chem. Eng. J.* **2014**, *248*, 79.
42. Shan, W.; Ren, F.; Zhang, Q.; Wan, L.; Xing, Z.; Lou, Z.; Xiong, Y. *J. Chem. Technol. Biotechnol.* **2015**, *90*, 888.
43. Ho, Y. S.; McKay, G.; Wase, D. A. J.; Foster, C. F. *Adsorp. Sci. Technol.* **2000**, *639*, 18.
44. Tang, L.; Fang, Y.; Pang, Y.; Zeng, G.; Wang, J.; Zhou, Y.; Deng, Y.; Yang, G.; Cai, Y.; Chen, J. *Chem. Eng. J.* **2014**, *254*, 302.
45. Ma, X.; Li, L.; Yang, L.; Su, C.; Wang, K.; Yuan, S.; Zhou, J. *J. Hazard. Mater.* **2012**, *209–210*, 467.
46. Yuan, Q.; Chi, Y.; Yu, N.; Zhao, Y.; Yan, W.; Li, X.; Dong, B. *Mater. Res. Bull.* **2014**, *49*, 279.
47. Liu, H.; Liu, W.; Zhang, J.; Zhang, C.; Ren, L.; Li, Y. *J. Hazard. Mater.* **2011**, *185*, 1528.
48. Nguyen, T. A.; Ngo, H. H.; Guo, W. S.; Zhang, J.; Liang, S.; Yue, Q. Y.; Li, Q.; Nguyen, T. V. *Bioresour. Technol.* **2013**, *148*, 574.
49. Wang, X.; Lü, S.; Gao, C.; Xu, X.; Zhang, X.; Bai, X.; Liu, M.; Wu, L. *Chem. Eng. J.* **2014**, *252*, 404.
50. Godelitsas, A.; Astilleros, J. M.; Hallam, K.; Harissopoulos, S.; Putnis, A. *Environ. Sci. Technol. 37*, 3351, **2003**.
51. Yang, L.; Li, Z.; Nie, G.; Zhang, Z.; Lu, X.; Wang, C. *Appl. Surf. Sci.* **2014**, *307*, 601.